ASSOCIAZIONE NAZIONALE ITALIANA DI
INGEGNERIA SISMICA
ANIDIS
Italian National Association of Earthquake Engineering

XVIII **CONVEGNO ANIDIS**
L'ingegneria sismica in Italia
ASCOLI PICENO 2019
15-19 Settembre

Strengthened thin clay masonry infills: experimental analysis and validation of verification procedures

Nicolò Verlato[a], Massimiliano Minotto[a], Marco Donà[a], Francesca da Porto[b]
[a] Department of Civil, Architectural and Environmental Engineering (ICEA), University of Padova, Via Marzolo 9, 35131 Padova, Italy
[b] Department of Geosciences, University of Padova, Via Gradenigo 6, 35131 Padova, Italy

ABSTRACT

Masonry infill walls present a brittle behaviour when subjected to combined in-plane and out-of-plane actions due to seismic events. This characteristic is even more pronounced in thin infill walls, often characterised by masonry units with high void ratio, horizontal hole arrangement and low compressive strength. Thin infills are mainly employed as internal partitions in current construction practice, but they can be found also as external enclosures in many existing R.C. frame buildings.

To overcome the intrinsic limits of this construction typology, three types of strengthening techniques are proposed: the first strengthening technique is characterised by the application of a bi-directional basalt mesh embedded in a special geo-polymeric plaster. The other two strengthening solutions consist of applying a fibre-reinforced lime-based plaster, and one of them is also provided with an additional bi-directional basalt mesh. To validate the effectiveness of the proposed solutions, eight combined in-plane and out-of-plane tests on full-scale R.C. infilled frames (one-bay, one-storey) have been performed. Specimens have been tested firstly imposing increasing in-plane cyclic displacements at the frame top beam, and secondly monotonically loading the infill in the out-of-plane direction.

This work presents an analysis of the obtained experimental results. The comparison with a reference plain masonry infill, tested in a previous experimental campaign, proves the effectiveness of the strengthening solutions in reducing infill damage and in increasing both the out-of-plane capacity and the deformability.

Furthermore, since the currently adopted Italian building code lacks specific recommendations on the evaluation of masonry infills out-of-plane capacity, this article proposes simplified procedures together with their validation against experimental results. These simplified procedures take into consideration existing damage due to in-plane deformations as well as the improvement provided by the application of strengthening techniques.

1 INTRODUCTION

Thin infill walls are mainly employed as internal partitions in current construction practice, but they can be found also as external enclosures in many existing R.C. frame buildings. They are characterised by percentages of voids, low strength and a brittle behaviour under horizontal or vertical loads. During earthquakes, the seismic action affects these non-structural walls and may cause the loss of building functionality accompanied by significant economic losses, and, additionally, an increased danger for human lives due to the partial or complete ejection of the infill. The potential infill ejection due to Out-Of-Plane (OOP) actions is incremented by the In-Plane (IP) damage of the masonry due to R.C. frame deformations, thus increasing their seismic vulnerability. The observation of the damages during the recent seismic events have highlighted the high seismic vulnerability of masonry enclosure walls, not only due to the inherent weakness of traditional unreinforced masonry but also due to a lack of a suitable and effective design procedure (Hak et al. 2012); the most frequent damage patterns have been studied by Braga et al. (2011) in order to identify the main causes of failure and linking them to commonly adopted construction rules.

This issue caused great interest in the scientific world and since 90s several experimental

campaigns were carried out to evaluate the performance of thin clay masonry infills subjected to combined In-Plane/Out-Of-Plane (IP/OOP) actions (Angel et al. 1994; Flanagan et al. 1999; Calvi et al. 2001; Calvi et al. 2004; Pereira et al. 2011; da Porto et al. 2013; Hak et al. 2014; Furtado et al. 2016). In these research activities a lot of different types of masonry infill were tested using clay units of different thickness, and testing different constructive solutions. All these experimental campaigns demonstrated that the OOP response of specimens worsens as the IP displacement demand, and thus the IP damage, increases. To overcome the masonry infill intrinsic vulnerabilities, different strengthening solutions may be used. The first studies on masonry infill walls seismic improvement proposed the use of Fibre-Reinforced Plastic (FRP) sheets to increase the OOP capacity (Tumialan et al. 2003; Saatcioglu et al. 2005). Later, the use of strengthening meshes, embedded in one or more layers of plaster, were developed; the effectiveness of these Textile Reinforced Mortars (TRM) for improving the Out-Of-Plane capacity of non-loadbearing masonry panels has been demonstrated by Calvi et al. (2001), Papanicolaou et al. (2007) and Valluzzi et al. (2014). EN 1998-1-1 recommends appropriate interventions to avoid brittle OOP failure in slender infill walls (slenderness greater than 15), mentioning the use of light wire meshes. Recent works have focused on the development of innovative systems for masonry infills (Markulak et al. 2013; Mohammadi et al. 2010; Totoev 2015; Preti et al. 2015; Nasiri et al. 2016) above all during the recently funded European INSYSME project (da Porto et al. 2016).

The aim of this work is to study the effectiveness of the proposed strengthening solutions for improving the IP and OOP behaviour of thin clay masonry infills. To achieve this objective an experimental campaign, consisting of material characterization tests and combined IP/OOP tests on real scale specimens with strengthened infill walls, has been performed.

Furthermore, since the currently adopted Italian building code lacks specific recommendations on the evaluation of masonry infills out-of-plane capacity, simplified procedures are proposed and validated against experimental results. These simplified procedures take into consideration existing damage due to in-plane deformations as well as the improvement provided by the application of strengthening techniques.

2 DESCRIPTION OF THE STRENGTHENING SOLUTIONS

To overcome the intrinsic limits of thin clay masonry walls, three types of strengthening techniques are proposed: the first strengthening technique is characterised by the application of a bi-directional basalt mesh embedded in a special geo-polymeric plaster. The other two strengthening solutions consist of applying a fibre-reinforced lime-based plaster, and one of them is also provided with an additional bi-directional basalt mesh.

To perform the experimental tests, the strengthening solutions were applied to masonry specimens or masonry infills made of thin clay blocks with dimensions of 250×120×250 mm (length × width × height), hole percentage of 60%, and arranged so as to have the holes in horizontal direction. According to EN 1996-1-1, clay units are of Group 4. Their average compressive strengths, parallel and orthogonal to the holes, are stated by the manufacturer according to EN 771-1 and equal to 8.0 N/mm^2 and 2.0 N/mm^2 respectively. The masonry blocks are laid with 12 mm thick horizontal joints and 8.8 mm thick vertical joints, filled with a mortar of declared class M5 (EN 998-2). Each wall was rendered with a 15 mm thick plaster layer on both sides, including the reinforcement layer, with a total wall thickness of about 150 mm. The experimental campaign involved a total amount of 8 real scale specimens that were reinforced with three different strengthening solutions identified as F, FB and RBB (). The first two solutions were applied directly on raw masonry surface whereas the latter was applied on an existing plaster layer. The above-mentioned solutions are characterized as follows:

1. Specimens F (Fibre plaster,): a 15 mm thick layer of fibre-reinforce plaster on each side of the infill. The plaster is of class CS III (EN 998-1), with quite fine grading (0÷1.8 mm) and made of pure NHL 3.5 (Natural Hydraulic Lime). In this solution, no strengthening mesh has been used.
2. Specimens FB (Fibre plaster and Basalt grid): based on the same type of plaster used in the previous solution (type F), in these specimens a balanced biaxial basalt fibre grid is embedded in the 15 mm thick fibre plaster layer on each side of the infill.
3. Specimens RBB (Render, Basalt grid and helicoidal Bars): a first plaster layer (shortly named R) of class CS II (EN 998-

1), with quite fine grading (0÷1.4 mm) and made of pure NHL 3.5, was applied directly on the masonry wall lateral surface. A second layer of plaster of class CS IV (EN 998-1) was applied on the first one with interposition of a balanced biaxial basalt fibre grid embedded be-tween the two layers. The second plaster type is a smoothing-levelling plaster type NHL 3.5 with the same grading of the initial one. The strengthening system was also anchored to the RC frame top beam with 8 mm diameter helicoidal stainless steel ties made of steel type AISI316.

Figure 1 shows the details of each strengthening solution.
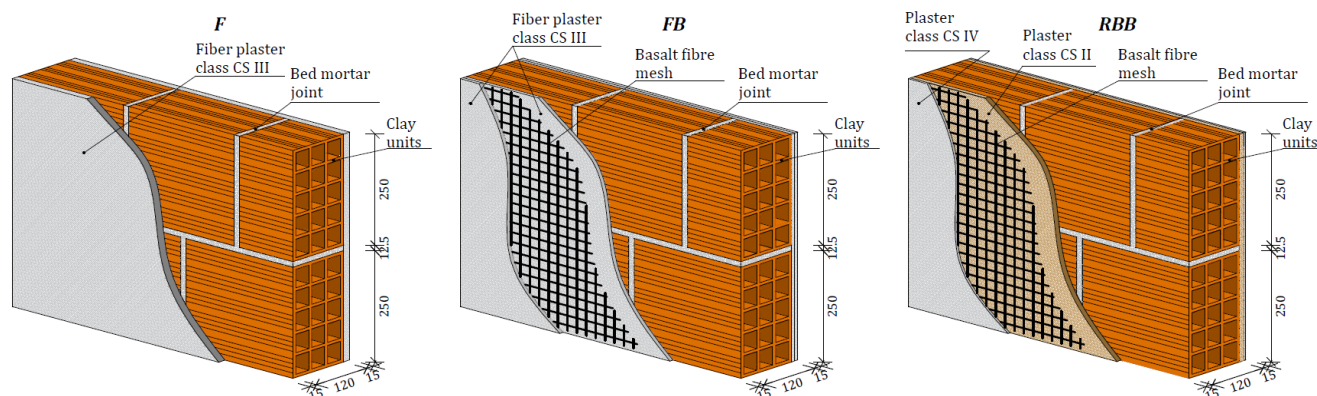
Figure 1. Detailed representation of the three analysed systems.

3 EXPERIMENTAL PROGRAM

3.1 Characterisation tests

Before the combined IP/OOP tests, a large experimental campaign was performed to characterize the mechanical properties of the materials. Flexural and compressive tests on masonry assemblages were conducted according to specific standard requirements. Two types of flexural tests are con-ducted, the first one applying the load directly on the mortar joint and the second one following a four-point bending approach, as per EN 1052-2 indications. In the first case, 9 masonry assemblages of 250x515x150 mm dimensions with plaster type R were tested. The load was applied in dis-placement control with a velocity of 0.5 mm/min. The typical failure mode occurs along the mortar joint as shown in Figure 2.a. In case of four-point bending tests (plane of failure parallel to bed joints), 4 specimens of dimensions 1300x390 mm for each type of strengthening solution (RBB, FB, F) were tested.

Each specimen was placed in a hydraulic press machine and tested with mono-tonic loading until failure (see test results in Table 2). Deflection of specimens was measured by six displacement sensors. In F type specimens collapse was sudden, immediately after achieving the maximum strength, showing a brittle behaviour. Conversely, RBB and FB specimens, due to the embedded of the reinforcing mesh, showed gradual failure (Figure 2.b). Further 12 masonry assemblages were tested in compression orthogonal to the clay blocks holes according to EN1052-1. The specimens were placed in a hydraulic press machine and the load was applied in displacement control with a velocity of 1.0 mm/min. The specimens of dimensions 775x780 mm were construct-ed with 3 types of strengthening solution (RBB, F, R). Typical failure modes are shown in Figure 2.c and Table 3 lists a summary of the results. Compression tests on clay units were not carried out, as the same blocks have already been tested during a previous experimental campaign (Valluzzi et al. 2014).
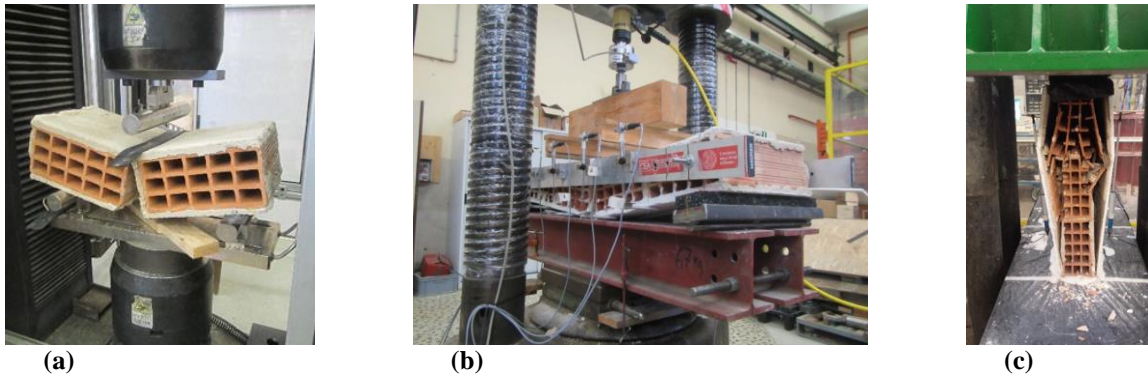
(a)   **(b)**   **(c)**

Figure 2. (a) Four-point bending tests, (b) flexural tests on mortar joints, (c) compressive tests.

Table 1. Flexural tests average results.

Specimen	Dimensionless bending moment [kN mm/mm]	Flexural strength [N/mm^2]
R	1.1	0.3
RBB	3.1	0.9
FB	3.1	0.8
F	2.7	0.7

Table 2. Compression tests average results.

Specimen	Max. load [kN]	Max. Compressive strength [N/mm^2]	Elastic modulus [N/mm^2]
RBB	357.6	2.9	4777
F	325.0	2.8	4752
R	293.0	2.7	4198

3.2 Combined In-Plane/Out-Of-Plane tests

The following Table 1 summarizes the configuration of the specimens and the type of experimental test. The number of each specimen name represents the maximum IP drift θ_{max} to which the sample is cyclically pushed before the OOP monotonic test.

3.2.1 Experimental Set-Up

The aim of the following experimental campaign is the evaluation of the response of eight specimens subjected to combined In-Plane and Out-Of-Plane actions. First, these tests were carried out to investigate the performance of the different strengthening solutions. In this way, it is significant to assess the state of damage of the infill walls with increasing values of IP inter-storey drifts. The second relevant aspect is the evaluation of the residual OOP capacity of the infill after its previously IP damage. The specimens were made of full-scale, one-bay and one-storey, RC frames (Figure 3) and were all entirely filled with thin masonry blocks. The frame

clear span and height were 4.15 m and 2.65 m respectively and the infill wall dimensions coincide with those values. Specimens were designed following the criteria described in da da Porto et al. (2013). Two actuators apply a constant vertical load of 200 kN over each beam-column node through a self-locking device hinged to the bottom beam. A servo-controlled hydraulic actuator, in correspondence of the beam-column node, applies horizontal In-Plane cyclic displacements of increasing amplitude. Each specimen was instrumented with 27 sensors:

– 11 potentiometric transducers plus 1 magneto strictive MTS transducer on the RC frame to measure IP deformations;
– 4 potentiometric transducers with return spring and 9 draw wire sensors on the infill wall to measure its global Out-Of-Plane deflection. The IP/OOP test set-up is shown in Figure 4

3.2.2 Experimental Procedure

The history of applied In-Plane displacements coincided with the following sequence of inter-storey drift: ±0.1%; ±0.2%; ±0.3%; ±0.4%;

±0.5%; ±0.6%; ±0.8%; ±1.0%; ±1.2%. According to Table 1, some specimens were pushed only until a value of drift 0.5%. The IP test was quasi-static with 3 cycles for each drift level with a maximum stroke speed of less than 0.5 mm/s. After the cyclic test, the specimen was brought back to null horizontal displacement to perform the Out-Of-Plane monotonic test on the infill until collapse.

After the removal of the crushed infill, the Bare Frame (BF) was In-Plane tested to evaluate its residual response. A simplified test procedure was adopted imposing a cyclical displacement history characterized by only two inter-storey drift targets (0.5% and 1.2%) with two cycles for the lower drift level and one for the 1.2% drift.
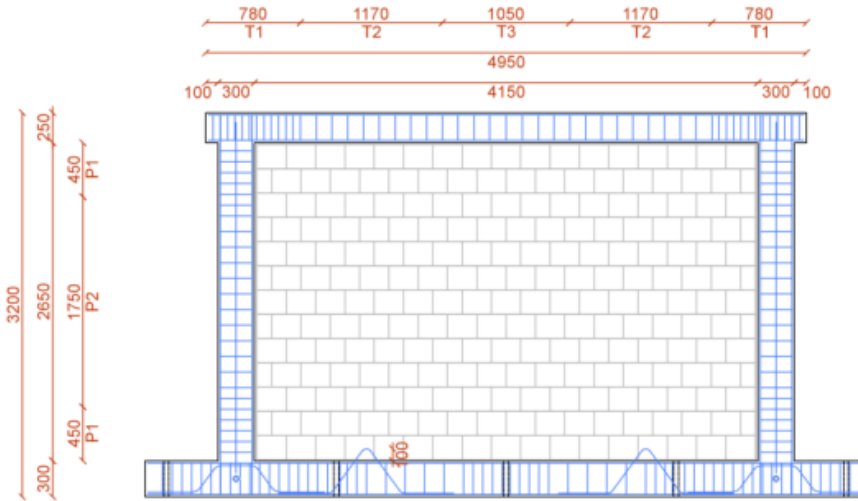
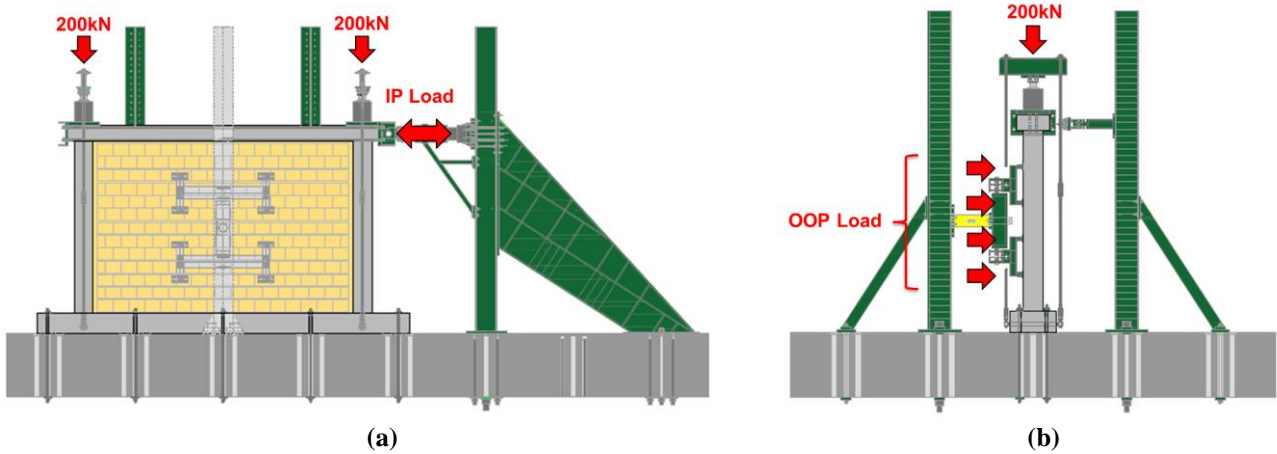Figure 3. Geometric characteristics of the infilled R.C. frames.

Figure 4. Experimental set-up: (a) details of In-Plane and (b) Out-Of-Plane push systems.

Table 3. Experimental specimen types.

| Specimen	Plaster type	Strengthening	Test type
F.00	-	Fibre-reinforced plaster of Class CS III	OOP
F.12			IP (θ_{max} 1.2%) + OOP
FB.00	-	Fibre-reinforced plaster of Class CS III + Basalt fibre grid	OOP
FB.05			IP (θ_{max} 0.5%) + OOP
FB.12			IP (θ_{max} 1.2%) + OOP
RBB.00	Class CS II	Class CS IV + Basalt fibre grid + Helicoidal stainless steel ties	OOP
RBB.05			IP (θ_{max} 0.5%) + OOP
RBB.12			IP (θ_{max} 1.2%) + OOP

4 EXPERIMENTAL RESULTS

4.1 In-Plane cyclic tests

As reported in Table 3, 5 specimens were In-Plane tested. FB.05 and RBB.05 were tested until 0.5% drift while F.12, FB.12 and RBB.12 until 1.2% drift. Figure 5 to Figure 7 show the hysteresis loops of all in-filled specimens (a) and the crack patterns at the end of In-Plane tests (b). Figure 8.a contains the IP envelope capacity curves of the infill walls calculated as the difference between the envelope curve at the third cycle (the most stabilized) of the infilled configuration and that of the bare frame. Figure 8.b shows the reduction of the stiffness for each infill type. Table 4 lists the principal information obtained by tests as the maximum IP capacity of specimens F_{max} and its corresponding drift level θ_{max}, the ultimate force F_{ult}, corresponding to a reduction of 20% of the maximum capacity, and its drift θ_{ult}. Finally, the maximum specimen stiffness K_{max}, always achieved at a drift of 0.1%, is re-ported.

As shown in Figure 5.a, specimen F.12 revealed the most relevant infill damage with large areas of detached plaster (mostly on the back side) and spalling of corner units at the end of the In-Plane test. The first crack opening along the infill-frame interface were observed at an IP drift of 0.2%. The hysteresis loops of the specimen were not completely symmetrical, due to a non-symmetrical damage on the reverse loading cycles. The same consideration can be extended to the cyclic behaviour of other specimens. The infill reached the maximum In-Plane capacity (229.7 kN, drift 0.3%; Table 4) without significative damage.

The FB and RBB strengthened specimens showed a completely different damage pattern with the detachment of some plaster portions from the masonry, as shown in Figure 6.a and Figure 7.a. The basalt fibre-reinforced grid prevented these portions from falling off the masonry wall and even stopped the falling of clay rubble from cracked units as already observed in RBB.12 (at the top right corner). For these specimens, the only visible cracks were at the interface between masonry infill wall and frame columns (Figure 6.b and Figure 7.b). Observing the envelope curves in Figure 8.a, the maximum capacity of FB.12 specimen (243.1 kN) was at the 0.3% drift whereas infill type RBB.12 showed a maximum load of 189.6 kN for a smaller IP drift equal to 0.2%. Indeed, both RBB specimens, among all tested specimens, showed a worst In-Plane behaviour, reaching lower peak strengths at lower drift levels. However, it should be observed that this retrofit solution gives to traditional infills a more ductility post-peak behaviour compared to un-strengthened ones (da Porto et al. 2015). In case of specimens with fibre-reinforced plaster, the presence of the mesh and a plaster of good mechanical properties, higher value of peak capacity is observed, after which the strength degradation was greater than the other infill solutions. Figure 8.b shows that stiffness degradation was similar for all tested specimens except for the F.12 one that, starting from 0.4% drift, showed a less degrading curve keeping a higher stiffness value at the end of the test.
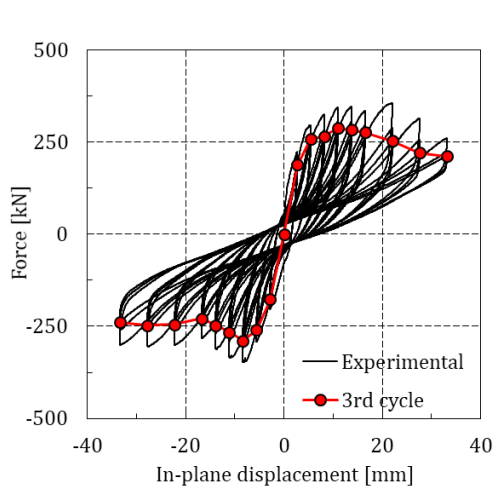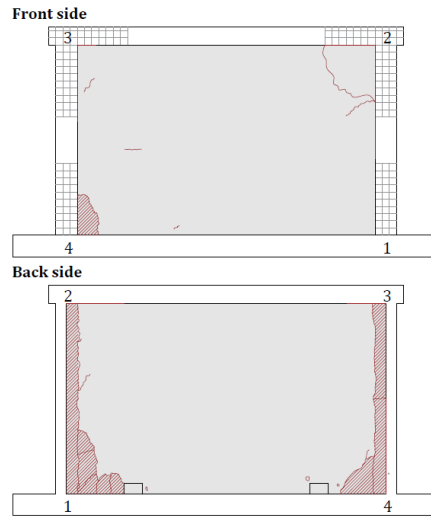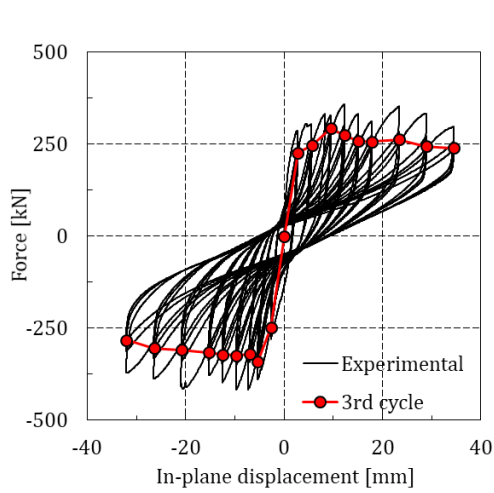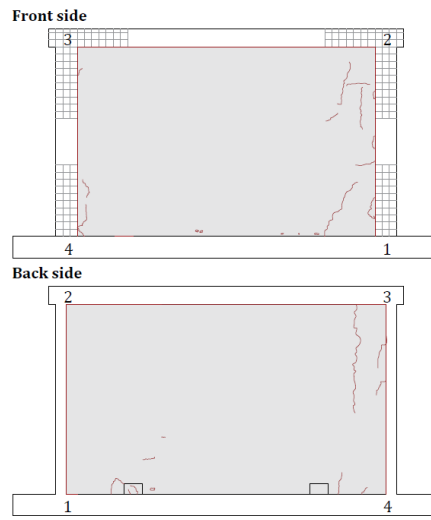
(a)   **(b)**

Figure 5. Specimen F.12: hysteresis loops and envelope curve at the 3rd cycle (a), and crack patterns at the end of the In-Plane test (b).
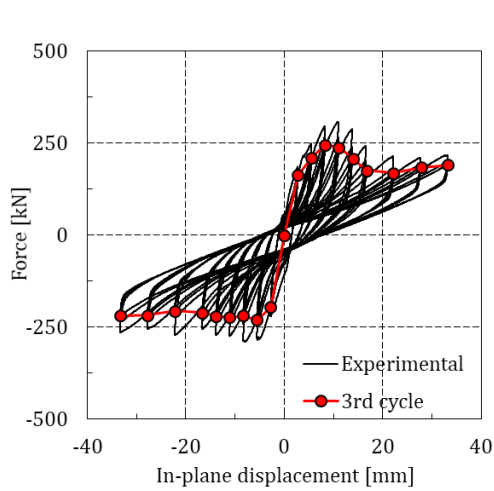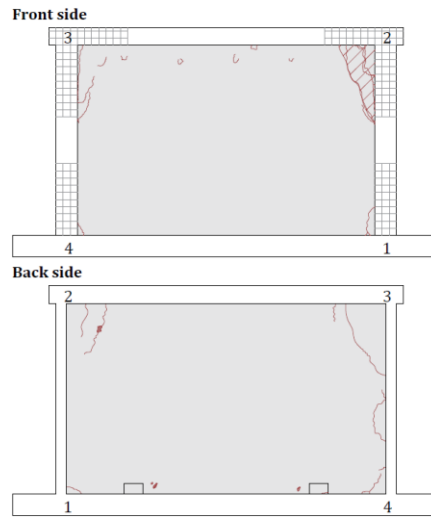

(a)   **(b)**

Figure 6. Specimen FB.12: hysteresis loops and envelope curve at the 3rd cycle (left), and crack patterns at the end of the In-Plane test (right).

(a)   **(b)**

Figure 7. Specimen RBB.12: hysteresis loops and envelope curve at the 3rd cycle (left), and crack patterns at the end of the In-Plane test (right).
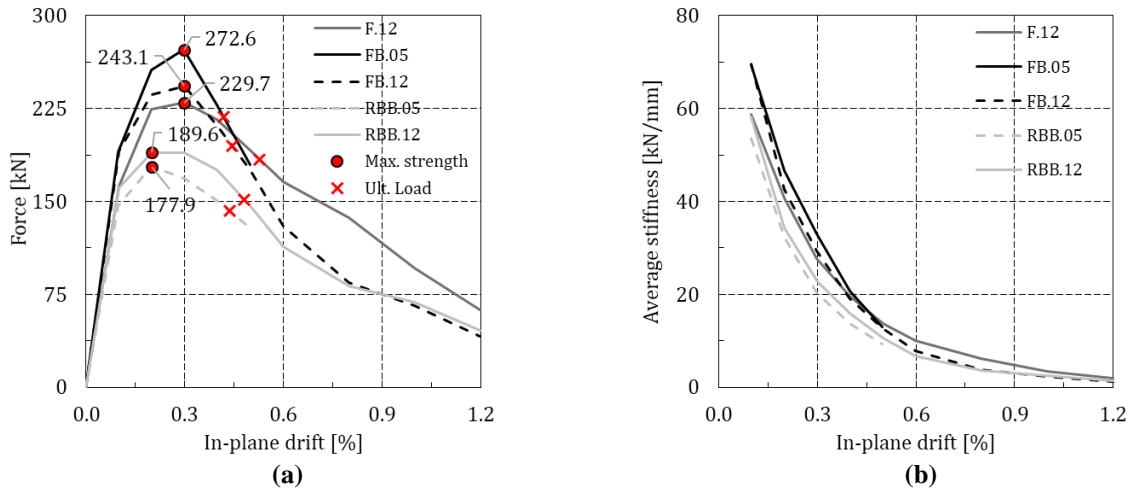
Figure 8. Comparison of load-drift envelope curves (a) and stiffness degradation (b) of all tested specimens.

Table 4. Summary of In-Plane test results.

Specimen	Max. load		Ultimate load		
	F_{max} [kN]	θ_{max} [%]	F_{ult} [kN]	θ_{ult} [%]	$\theta_{ult}/\theta_{max}$ [-]
F.12	229.7	0.30	183.8	0.53	1.77
FB.05	272.6	0.30	218.1	0.44	1.41
FB.12	243.1	0.30	194.5	0.45	1.49
RBB.05	177.9	0.20	142.3	0.44	2.20
RBB.12	189.6	0.20	151.6	0.48	2.41

4.2 Out-Of-Plane monotonic tests

Figure 9 compares all the Out-Of-Plane load-displacement curves and lists the main test results in terms of maximum OOP strength F_{max} and its corresponding displacement δ_{max}. Figure 8 shows the typical collapse modes of the infills at the end of the OOP experimental test. The curves in Figure 7 shows a degradation of the maximum OOP strength and of the stiffness as the IP damage increased for all infill types. The In-Plane damage and the resulting degradation of the mechanical properties of the masonry influenced the OOP behaviour of the infills. Un-strengthened specimen F.00 showed an initial stiffness similar to that of the FB.00 due to the use of the same plaster type however, after the formation of the first cracks (at around 30 kN load), FB.00 specimen had a more rigid behaviour due to the reinforcing mesh. RBB.00 specimen showed an intermediate behaviour between the previous ones. Indeed, the presence of two types of plaster (one with poor mechanical properties) induced a lower initial stiffness compared to that of the FB.00 specimen and the mesh gives an intermediate hardening branch until the reaching of the peak strength

(101.31 kN). In detail, RBB.00 specimen reached the maximum strength for a greater value of OOP deflection (12.14 mm) compared to that of FB.00 (5.35 mm). F.00 specimen showed a strength degrading branch after its maximum capacity (90.05 kN) until the OOP fragile collapse with sudden and uncontrolled ejection of entire portions of masonry (Figure 10.a).Conversely, FB.00 and RBB.00 had a more controlled collapse, without the expulsion of masonry portions. After the reaching of the peak strength, these specimens showed a gradual damaging of the upper or lower interface allowing the masonry panel to rigidly rotate in the Out-of-Plane until collapse (Figure 10.b and Figure 10.c). After the IP damage, specimen F.12 reached the OOP maximum capacity (59.53 kN) showing a reduction of about 30% compared to that of F.00 with a subsequent fragile failure mode. In the case of strengthened infill walls, the increment of the IP damage induced a reduction of the maximum strength and, typically, an increment of the OOP displacement corresponding to the peak point, due to both the reduction of stiffness and the damage of the infill-frame masonry interfaces. In general, the capacity curves show significant degradation of the OOP

strength already at low IP deformations (i.e. 0.5% drift); however, it does not significantly increase for higher IP drift levels. FB.12 specimen shows an anomalous behaviour, because its strength is higher than that of FB.05 which was tested for a lower IP damage. This is probably due to a much more accurate (and so less representative) specimen construction, which was the consequence of a previous failed test on the same specimen.

Finally, Table 5 lists the values of the equivalent Out-Of-Plane acceleration reached by each infill type (a_{eq}). It is important to underline that the seismic action may reduce the actual OOP strength, compared with those experimentally obtained by means of the adopted quasi-static monotonic test. Indeed, the dynamic effects may anticipate the collapse of single masonry portions, particularly on those walls in which concurrent IP frame displacements cause severe damages.
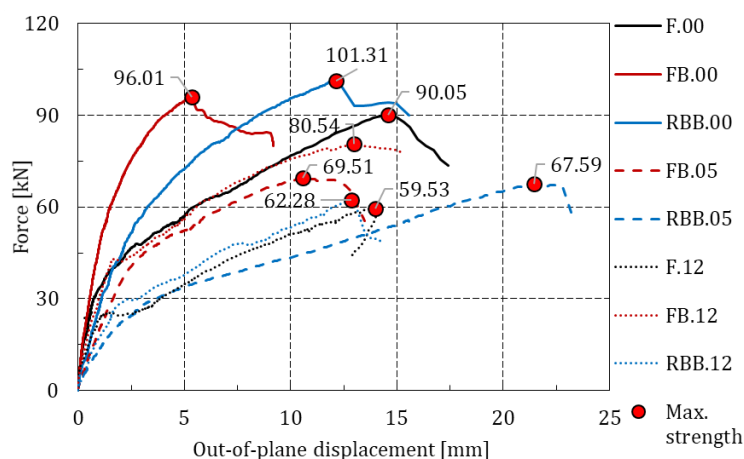

Figure 9. Comparison of the Out-Of-Plane load-displacement curves for all specimens.

Table 5. Summary of Out-Of-Plane test results.

Specimen	Out-Of-Plane Capacity			Failure mode
	F_{max} [kN]	δ_{max} [mm]	a_{eq} [g]	
F.00	90.05	14.60	6.91	Material ejection
F.12	59.53	13.97	4.57	Material ejection
FB.00	96.01	5.35	7.36	Controlled
FB.05	69.51	10.58	5.33	Controlled
FB.12	80.54	13.00	7.46	Controlled
RBB.00	101.31	12.14	7.18	Controlled
RBB.05	67.59	21.47	4.79	Controlled
RBB.12	62.28	12.84	4.42	Controlled

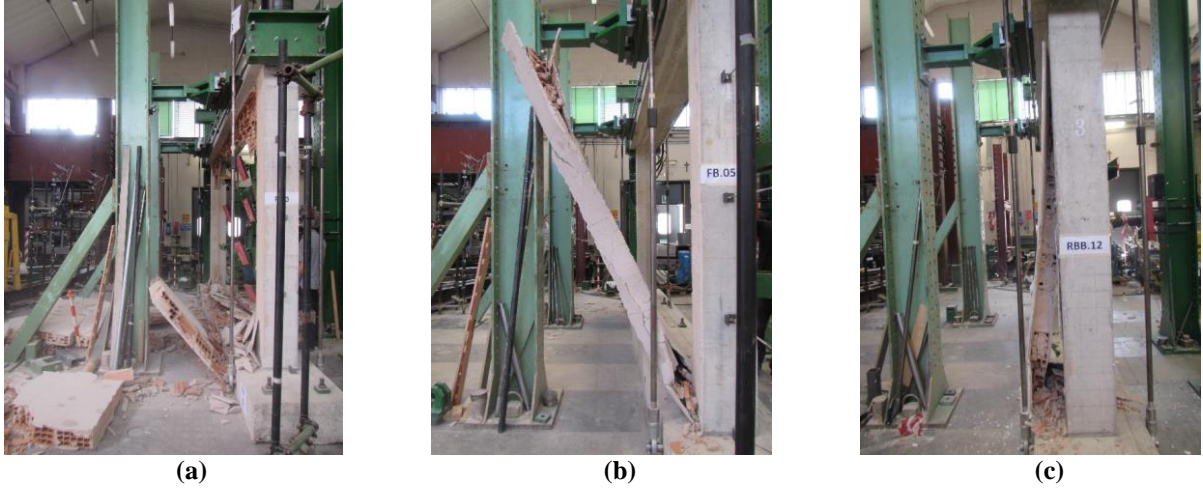**(a)**   **(b)**   **(c)**

Figure 10. Out-Of-Plane failure mode for F type specimens (a), FB type specimens (b) and RBB type specimens (c).

4.3 *In-Plane/Out-Of-Plane interaction*

As observed by experimental combined tests, the Out-Of-Plane maximum strength reduces as the In-Plane damage increases. According to Verlato et al. (2014), an OOP strength reduction factor α can be introduced as reported in equation (1).

$$f_{m,red} = \alpha f_m \qquad (1)$$

The coefficient α, function of the masonry type and of the IP damage level, is defined in equation (2).

$$\alpha = \frac{1}{a}\left[(a-1)e^{-(b \cdot \theta_{IP})^2} + 1\right] \qquad (2)$$

Where a=1.6, b=2.5 and θ_{IP} is the In-Plane drift. The strength degradation curve shown in the graph in Figure 11 was obtained by multiplying the previous reduction coefficient by the average OOP strength value reached by un-damaged infills (in detail, specimens F.00, FB.00 and RBB.00). The maximum strength degradation is around 30% at the 1.2% IP drift. FB.12 specimen reached a peak strength value beyond expectations as previously observed on its Out-Of-Plane capacity curve.
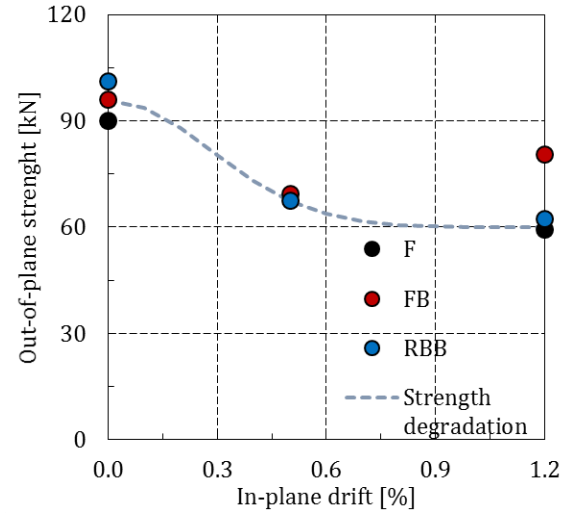

Figure 11. Out-Of-Plane strength degradation due to In-Plane damage.

5 DESIGN FORMULATIONS

According to DM 17/01/2018, the OOP capacity of non-structural elements must be greater than the seismic demand corresponding to the considered design limit state. The effects of the seismic action on non-structural elements can be determined by applying a horizontal force F_a defined in equation (3):

$$F_a = \frac{S_a W_a}{q_a} \qquad (3)$$

Where Fa is the horizontal seismic force acting in the centre of mass of the non-structural element, resulting from the distributed forces proportional to mass, W_a is the weight of the wall, and q_a is the behaviour factor (equal to 2 according to Circular 21/01/2019 n. 7, Table C7.2.I), S_a is the maximum

OOP acceleration, calculated according to Circular 21/01/2019 n. 7 (§C7.2.3) by means of response spectra or through simplified formulations of proven validity. Therefore, the OOP seismic action can be represented by the horizontal force F_a distributed along the free height of the wall h_0 (Figure 12).
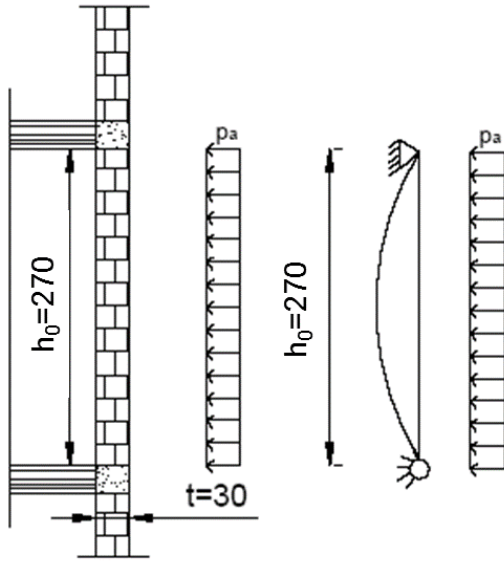

Figure 12. Distribution of seismic forces along the infill height.

5.1 Out-Of-Plane arch mechanism

According to EN 1996-1-1, the Ultimate Limit State verification of masonry walls built in adherence to structural elements (i.e. capable of bearing the thrust due to the formation of an arch mechanism) can be carried out assuming that a horizontal or vertical arch develops within the wall thickness. The analysis can be carried out by assuming the configuration of a three-hinged arch with an arch support footprint at the extremities and on the central hinge equal to 0.1 times the thickness of the wall t_w (Figure 13).
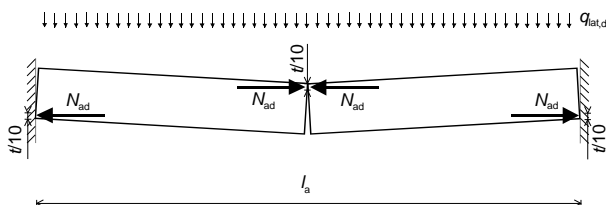

Figure 13. Development of the arch mechanism due to lateral forces.

According to the formation of the arch mechanism, the resistant moment M_r of the masonry wall can be calculated as defined by equation (4), where f_d is the design strength of the masonry.

$$M_r = 0.9t_w f_d 0.1t_w = 0.09 f_d t_w{}^2 \qquad (4)$$

From the comparison between soliciting moment and resistant moment it is possible to obtain the lateral design strength as defined by equation (5):

$$q_{lat,d} = 0.72 f_d \left(\frac{t_w}{h_w}\right)^2 \qquad (5)$$

where h_w is the height of the wall.
This load, for the verification to the Ultimate Limit State, should be compared to the lateral load induced by the seismic action.

It should be noted that the OOP arch mechanism formulation is provided by EN 1996-1-1 with a unitary factor, instead of 0.72. As included in the regulation (§6.3.2), the formulation entail an overestimation of the lateral strength of about 50% (defined in relation to masonry made with Group 1 blocks). For the analysed masonry infills, it is considered more reliable to apply the formulation proposed in this paper, which is derived from pure mechanical considerations and in agreement with Drysdale et al. (1999).

5.2 Evaluation of the strength contribution of the reinforcement layer: arch mechanism with simplified reinforcement contribution

According to Morandi et al. (2013), and analysing previous experimental test results (Calvi et al. 1999; Calvi et al. 2001), the OOP strength of thin masonry infill walls with external reinforcement can be calculated by adding the reinforcement contribution to the whole resistant moment given by the arch mechanism. The resistant moment of the reinforcement is calculated through a simplified approach considering a neutral axis depth equal to that used for the calculation of the arch mechanism. In particular, the contribution given by the reinforcement is defined by equation (6), where A_s and f_{yd} are, respectively, the whole cross-section area and the design yield strength of the vertical reinforcement.

$$M_r = 0.9 t_w A_s f_{yd} \qquad (6)$$

Expressing the resistant moment per unit length of the wall (L_w), the OOP design strength can be calculated according to equation (7).

$$q_{lat,d} = 0.72 f_d \left(\frac{t_w}{h_w}\right)^2 + 7.2 \frac{t_w}{L_w h_w{}^2} A_s f_{yd} \qquad (7)$$

5.3 Validation of the proposed formulations

The histogram in Figure 14 shows a comparison among the Out-Of-Plane experimental strength values and those calculated through the proposed formulations. The experimental results refer to the capacity of un-damaged masonry panels, reinforced with the three analysed reinforcement solutions (F, FB and RBB). It should be noted that, for comparison purposes, calculations were carried out considering the mean mechanical values of the materials, therefore, neglecting partial safety coefficients. Furthermore, calculated strength values, consistently with experimental conditions, are obtained by evaluating the out-of-plane thrust applied along four load lines.

It can be observed that the plain arch formulation, in blue in the histogram, neglecting the contribution offered by surface reinforcements, in all cases abundantly underestimates the experimental strength with deviations ranging from 33% (F) to 40% (RBB).

A better approximation of the experimental results can be obtained with the simplified approach: the contribution offered by the external reinforcement system is added to the strength offered by the arch mechanism. It should be noted that for the calculations in the case of fibre-reinforced plaster the area and the yield strength of the reinforcement are considered to be, respectively, the whole cross section of the applied fibre plaster and the tensile strength of the plaster.

It can be seen that the simplified formulation proposed by Morandi et al. (2013) gives results that are very close to experimental ones, although it tends to provide slightly overestimated values, with deviations of about, at most, 5%.
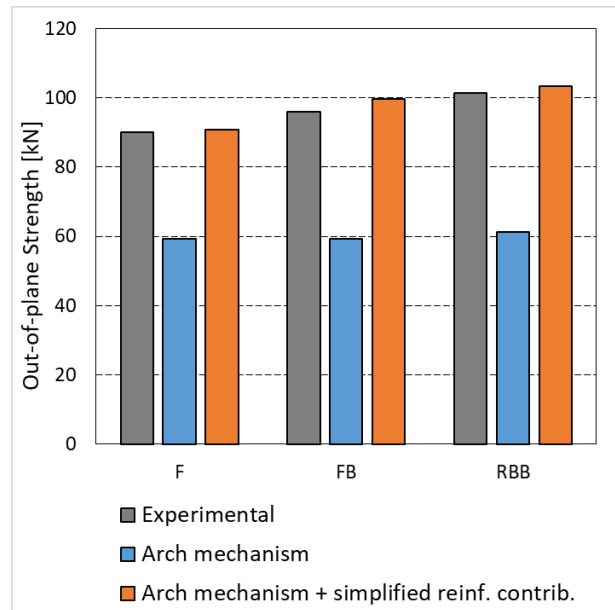

Figure 14. Comparison among the experimental strength values and the proposed formulations.

6 CONCLUSIONS

Considering the results of IP tests, embedding a strengthening mesh on the external plaster layers produces a confinement effect which reduces the In-Plane damage of the infill wall. The basalt fibre grid cannot prevent the crushing of masonry units and the detachment of plaster portions, but it has a beneficial effect, preventing the expulsion of masonry and plaster portions. As observed, all the specimens reached the IP peak strength at drift levels between 0.2% and 0.3%. The experimental results on weak masonry infill walls confirms that a lower drift value for the Damage Limitation Limit State should be considered instead of that proposed by standards requirements (as already observed by Hak et al. 2012 and Donà et al. 2017). The initial stiffness of the wall is slightly higher in case of strengthening solutions based on fibre-reinforced plaster, compared to the RBB one, due to the better mechanical properties of the plaster. This is associated with higher values of In-Plane peak strength. In the rehabilitation of existing buildings, strengthening solutions type F and FB should be used to obtain high values of strength and a gradual degradation of mechanical properties as IP damage increases. The reinforcing grid has a further beneficial effect influencing significantly the Out-Of-Plane response of the infill wall. Indeed, the mesh prevents brittle collapse to occur, which is of the utmost importance during seismic events. To evaluate the

contribution of reinforcement systems on the overall Out-Of-Plane strength of masonry infill walls a simplified calculation approach, originally proposed by Morandi et al. (2013), was considered. The validation against experimental results show a good reliability of the proposed method, that, although slightly overestimating them by not more than 5%, adequately approximates experimental values.

7 ACKNOWLEDGEMENTS

REFERENCES

Angel, R. E., Abrams, D. P., Shapiro, D., Uzarski, J., Webster, M., 1994. Behavior of reinforced concrete frames with masonry infill walls. University of Illinois at Urbana-Champaign.

Braga, F., Manfredi, V., Masi, A., Salvatori, A., Vona, M., 2011. Performance of non-structural elements in RC buildings during the L'Aquila, 2009 earthquake. *Bulletin of Earthquake Engineering*, 9(1), 307–324.

Calvi, G. M., Bolognini, D., 1999. Seismic Response of R.C. Frames Infilled With Weakly Reinforced Hollow Masonry Panels. Pavia, Italy.

Calvi, G. M., Bolognini, D., 2001. Seismic Response of Reinforced Concrete Frames Infilled With Weakly Reinforced Masonry Panels. *Journal of Earthquake Engineering*, 5(March 2014), 153–185.

Calvi, G. M., Bolognini, D., Penna, A., 2004. Seismic Performance of Masonry-Infilled RC Frames: Benefits of Slight Reinforcements. In *6th Portoguese Congress on Seismology and Earthquake Engineering*,

Circolare 21/01/2019 n. 7, 2019. Istruzioni per l'applicazione dell'«Aggiornamento delle "Norme tecniche per le costruzioni"» di cui al decreto ministeriale 17 gennaio 2018. 1, 1–51.

DM 17/01/2018, 2018. Aggiornamento delle 'Norme Tecniche per le Costruzioni' - NTC 2018. 1–198.

Donà, M., Minotto, M., Saler, E., Tecchio, G., da Porto, F., 2017. Combined in-plane and out-of-plane seismic effects on masonry infills in RC frames. *Ingegneria Sismica, International Journal of Earth-quake Engineering*, 34(3), 157–173.

Drysdale, R. G., Hamid, A. A., Baker, L. R., 1999. Masonry Structures: Behaviour and Design, 3rd edition. Boulder, Colorado, US: The Masonry Society.

EN 1052-2, 2001. Methods of test for masonry - Determination of flexural strength.

EN 1996-1-1, Design of masonry structures - Part 1-1: General rules for reinforced and unreinforced masonry structures.

EN 1998-1, Design of structures for earthquake resistance Part 1: General rules, seismic actions and rules for buildings.

EN 771-1, Specification for masonry units Part 1: Clay masonry units.

EN 998-1, Specification for mortar for masonry - Part 1: Rendering and plastering mortar.

EN 998-2, Specification for mortar for masonry - Part 2: Masonry mortar.

Flanagan, R. D., Bennett, R. M., 1999. Bidirectional Behavior of Structural Clay Tile Infilled Frames. *Journal of Structural Engineering*, 125(3), 236–244.

Furtado, A., Rodrigues, H., Arêde, A., Varum, H., 2016. Experimental evaluation of out-of-plane capacity of masonry infill walls. *Engineering Structures*, 111, 48–63.

Hak, S., Morandi, P., Magenes, G., 2014. Out-of-plane Experimental Response of Strong Masonry Infills. *2nd European Conference on Earthquake …*, .

Hak, S., Morandi, P., Magenes, G., Sullivan, T. J., 2012. Damage Control for Clay Masonry Infills in the Design of RC Frame Structures. *Journal of Earthquake Engineering*, 16(sup1), 1–35.

Markulak, D., Radić, I., Sigmund, V., 2013. Cyclic testing of single bay steel frames with various types of masonry infill. *Engineering Structures*, 51(8), 267–277.

Mohammadi, M., Akrami, V., 2010. An engineered infilled frame: Behavior and calibration. *Journal of Constructional Steel Research*, 66(6), 842–849.

Morandi, P., Hak, S., Magenes, G., 2013. Simplified Out-of-plane Resistance Verification for Slender Clay Masonry Infills in RC Frames. In *XV Convegno ANIDIS - 'L'INGEGNERIA SISMICA IN ITALIA'*, Padova

Nasiri, E., Liu, Y., 2016. Experimental study of the effect of interfacial gaps on the in-plane behaviour of masonry infilled RC frames. In C. Modena, F. da Porto, & M. R. Valluzzi (eds) *16th International Brick and Block Masonry Conference*, Padova, Italy: Taylor & Francis

Papanicolaou, C. G., Triantafillou, T. C., Papathanasiou, M., Karlos, K., 2007. Textile reinforced mortar (TRM) versus FRP as strengthening material of URM walls: out-of-plane cyclic loading. *Materials and Structures*, 41(1), 143–157.

Pereira, M. F. P., Pereira, M. F. N., Ferreira, J. E. D., Lourenço, P. B., 2011. Behavior of masonry infill panels in RC frames subjected to in plane and out of plane loads. *Amcm2011 - 7th International Conference on Analytical Models and New Concepts in Concrete and Masonry Structures*, .

da Porto, F., Guidi, G., Dalla Benetta, M., Verlato, N., 2013. Combined In-Plane/Out-of-Plane Experimental Behaviour of Reinforced and Strengthened Infill Masonry Walls. In The Masonry Society (ed) *12th Canadian Masonry Symposium*,

da Porto, F., Guidi, G., Verlato, N., Modena, C., 2015. Effectiveness of plasters and textile reinforced mortars for strengthening clay masonry infill walls subjected to combined in-plane/out-of-plane actions / Wirksamkeit von Putz und textilbewehrtem Mörtel bei

der Verstärkung von Ausfachungswänden aus Ziegel. *Mauerwerk*, 19(5), 334–354.

da Porto, F., Verlato, N., Guidi, G., Modena, C., 2016. The INSYSME project : Innovative construction systems for earthquake resistant masonry infill walls. *In Brick and Block Masonry – Trends, Innovations and Challenges - 16th International Brick and Block Masonry Conference*, 1, 1173–1178.

Preti, M., Migliorati, L., Giuriani, E., 2015. Experimental testing of engineered masonry infill walls for post-earthquake structural damage control. *Bulletin of Earthquake Engineering*, 13(7), 2029–2049.

Saatcioglu, M., Serrato, F., Foo, S., 2005. Seismic Performance of Masonry Infill Walls Retrofitted With CFRP Sheets. *Proceedings of 7th International Symposium on Fiber-Reinforced Polymer (FRP) Reinforcement for Concrete Structures, ACI Special Publication*, 230, 341–354.

Totoev, Y. Z., 2015. Classification of SIM infill panels. *Mauerwerk*, 19(1), 74–79.

Tumialan, J. G., Galati, N., Nanni, A., 2003. Fiber-Reinforced Polymer Strengthening of Unreinforced Masonry Walls Subject to Out-of-Plane Loads. *American Concrete Institute (ACI) Structural Journal*, 100(3), 321–329.

Valluzzi, M. R., da Porto, F., Garbin, E., Panizza, M., 2014. Out-of-plane behaviour of infill masonry panels strengthened with composite materials. *Materials and Structures*, 47(12), 2131–2145.

Verlato, N., Guidi, G., da Porto, F., 2014. Experimental testing and numerical modelling of infill masonry walls subjected to in-plane damage. *9th International Masonry Conference*, 10.